Available online at www.sciencedirect.com

ScienceDirect

Procedia Engineering 10 (2011) 1532–1537

Engineering Procedia

ICM11

Off-Axis Properties of Cross-Ply Metal Matrix Composites at Quasi-Static and High Strain Rates

I. W. Hall[1]* A. Tasdemirci[2] and Ali Kara[2]

[1]*Department of Mechanical Engineering, University of Delaware, Newark, DE 19716, U.S.A.*
[2]*Department of Mechanical Engineering, Izmir Institute of Technology, Izmir, Turkey*

Elsevier use only: Received date here; revised date here; accepted date here

Abstract

Cylindrical samples of a 0/90° cross-ply Nextel 610^{TM}/Al-6061 (~55V_f%) metal matrix composite have been subjected to compression testing at quasi-static and high strain rates over a range of angles between 0° and ±45° with respect to the principal fiber directions. The results, combined with testing in the longitudinal, transverse and through thickness directions, provide a detailed description of the response of such composites over a wide range of orientations. In addition, metallographic and fractographic studies along with high-speed camera records provide detailed information about the sequence of deformation events leading to fracture. Results confirm not only the strong dependence of mechanical properties upon orientation but also the critical importance of precise fiber alignment and processing in obtaining the desired theoretical properties. A misalignment of 10° was sufficient to cause an ~40% decrease in maximum stress and the properties were found to vary by >70% over the orientations investigated. The high strain rate properties were generally significantly greater than those measured quasi-statically. A numerical model based on the commercial explicit finite element code LS-DYNA was used to investigate the compressive deformation and fracture of the composite. Experimental results are compared with those of the numerical model.

Keywords: metal matrix composite; compression; off-axis properties; numerical model.

1. Introduction

Metal matrix composites (MMC's) are now quite mature materials and may be used in areas involving abrasion, wear and high tensile or compressive loading. Applications of MMC's in armor are also being increasingly explored and such uses require a detailed knowledge of the material behavior at both quasi-static and high strain rates. Considerable research and data generation has been carried out concerning the properties of a range of MMC's in simple configurations with fibers aligned, e.g., in the longitudinal and/or transverse directions [1-4]. The mechanical properties in these orientations are generally well understood and can also be modeled quite successfully. It has also been known for a long while [5,6] that even small deviations from precise alignment can

* Corresponding author. Tel.: +1 302 831 2421; fax: +1 302 831 3619
E-mail address: halliw@udel.edu

Selection and peer-review under responsibility of ICM11 doi:10.1016/j.proeng.2011.04.256

lead to a rapid decline in properties which makes aligned composites very sensitive to the perfection of manufacturing and lay-up details.

However, relatively few data exist concerning the behavior of MMC's when cross-plied or in off-axis directions. The present research was initiated, therefore, so as to begin providing a foundation upon which to develop future MMC's in which the fiber architecture may be tailored according to the intended application. The study comprises a combination of approaches in which selected experiments guide the development of numerical models.

2. Experimental & Numerical

The MMC samples were taken from a single plate of Nextel 610^{TM}/Al-6061 measuring 152 x 76 x 13 mm. The plate was laid-up in the 0/90° orientation with a fiber volume fraction of approximately 55%. The respective alumina fiber layers were ~250μm thick, yielding a total of 52 layers through the plate thickness. The plate was then sliced into ~10mm wide bars inclined at 0°, 10°, 20°, 30°, 40° & 45° to the long transverse axis. The side faces of these bars were then ground and diamond polished to ensure that they were flat and parallel before core drilling ~9.6 mm diameter cylindrical test samples from the bars. This procedure yielded at least 7 samples with an aspect ratio of approximately 1:1 from each bar, sufficient for multiple tests at each orientation.

Before testing, the side-surfaces of each sample were finely polished to remove possible stress-raisers and to give better visibility for picture and video quality. Samples were tested quasi-statically at an initial strain rate of 4 x 10^{-4} s^{-1} in a screw-driven Instron machine. High strain rate tests were performed on a split Hopkinson bar apparatus. The bars were 19.6 mm in diameter, and the striker, incident and transmitter bars were 3570, 1785 and 360 mm in length respectively. The use of a half-length transmitter bar avoided the possibility of multiple impacts and this was confirmed by the high-speed photography. The ends of the bars were protected from indentation due to the stiff fiber bundles through the use of impedance matched high strength maraging steel end-caps which were replaced with newly machined and polished ones for each test. Tests were all performed with a striker bar velocity of approximately 20m.s^{-1}, producing a nominal initial strain rate of 800 s^{-1}. Since many of the samples showed limited strain to failure, pulse shapers were employed in order to better capture details of the initial stress increases and data reduction was performed using the two-wave approach.

High-speed photography was used during the high strain rate tests to follow the processes of damage accumulation and fracture initiation. Also, after testing, representative samples were prepared either for cross-sectional optical microscopy or for scanning electron microscopy in order to further study details of the fracture processes.

For the numerical modeling portion of the study, the commercial finite element code LS-DYNA 971 was used to model Split Hopkinson Pressure Bar experiments. The MAT-162 progressive failure model was used in order to model damage progression and delamination in the samples. This model is based on the principle of progressive failure of Hashin [7] and damage mechanics of Matzenmiller *et al*. [8] which control strain-softening behavior after failure. Further details of the model are presented in a companion paper in these proceedings [9]: note, however, that the material parameters are specific to each specimen and lay-up.

3. Results

3.1. Quasi-static Testing

Results of the quasi-static tests are summarized below in Table 1 and indicate, as anticipated, a clear and rapid decrease of compressive fracture strength with increasing deviation from the basic 0/90° orientation. Typical stress *vs.* strain curves are presented in Fig. 1. It is noted that the strain to failure increases markedly with deviation from the 0/90° orientation and that this increase is accompanied by the appearance of increasingly well separated yield

and fracture (or maximum) stresses. It is seen, however, that the yield stress decreases to 40° and then recovers somewhat up to 45°.

Table 1. Quasi-static compression test results

Orientation (with respect to 0/90° axis)	Yield Stress (MPa)	Maximum Stress (MPa)	Strain at Max. Stress (%)
0°	n/a	2106 ± 87	6.3 ± 1.8
10°	n/a	1168 ± 125	6.6 ±0.6
20°	432 ± 31	638 ± 4	8.0 ±1.4
30°	359 ± 55	501 ± 126	11.8 ±1.9
40°	252 ± 20	499 ± 19	17.8 ± 2.3
45°	405	595	28.5 ± 4.5

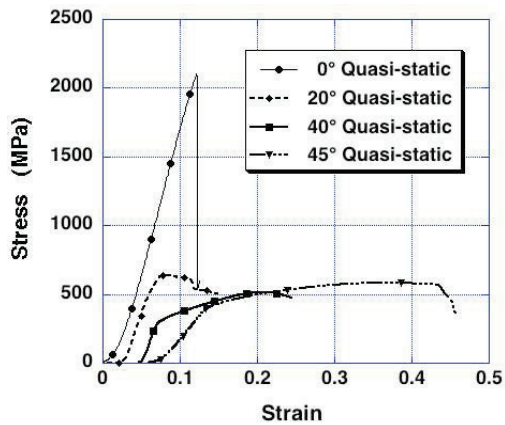

Fig. 1: Comparison of quasi-static stress-strain curves for different orientations. (For clarity, each origin is offset by a strain of 0.02 relative to the prior curve.)

3.2. High Strain-Rate Testing

Results of high strain rate tests are presented below in Table 2 and again show a clear and rapid decrease of compressive fracture strength with increasing deviation from the basic 0/90° orientation.

Table 2. High strain-rate compression test results

Orientation (with respect to 0/90° axis)	Maximum Stress (MPa)	Strain at Max. Stress (%)
0°	2225 ± 90	2.5 ± 0.12
10°	1390 ± 20	1.8 ± 0.1
20°	925	6.3 ± 0.12
30°	598	11.4 ± 5.3
40°	522	16.4 ± 4.3
45°	247	18.7 ± 3.2

Typical stress *vs.* strain curves are presented in Fig. 2(a). It is noted again that the strain to failure increases markedly with deviation from the 0/90° orientation although, distinct from the quasi-static results, there is a small

separation between the yield and maximum stresses at first and the maximum stresses follows smoothly and immediately after an initial yielding event. At larger deviations, the stress *vs.* strain curves were not monotonic but began to exhibit a sequence of loading/unloading events with each successive peak reaching a higher stress than the previous one until, ultimately, failure occurred. These peaks were not associated with possible Pochhammer-Chree waves arising from reverberations within the bars and corresponded, therefore, to actual physical events occurring within the samples. Figure 2(b) depicts graphically the decline of maximum stress with misorientation for both strain rates.

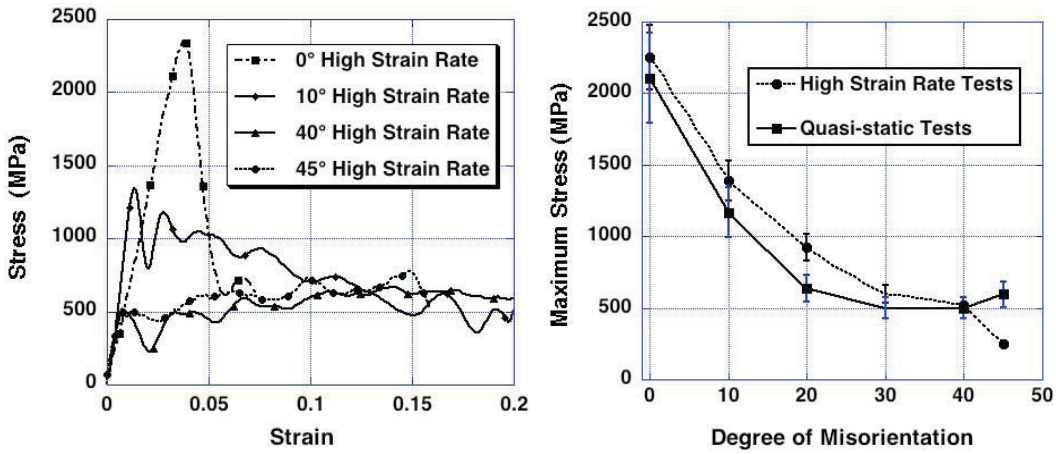

Figure 2: (a) Comparison of high strain-rate stress-strain curves for several orientations; (b) summary of quasi-static and high strain rate data showing decline of maximum stress with misorientation.

3.3. Fractography

Selected frames from high-speed photographic sequences of representative tests are presented below as Figures 3(a) & (b) and illustrate the general features of the deformation and fracture events. Fig. 3(a) shows that for the 0° orientation the principal event is the sudden onset of major splitting between the layers beginning at the base of the cylindrical sample followed afterwards by brooming. However, when the orientation changed by as few as 10°, Fig. 3(b), the mode of fracture changed quite distinctly and consisted solely of brooming during much of the deformation. This was followed by only minor amounts of layer splitting towards the end of the test. At 20° orientation, Fig. 3(c), deformation and fracture was much more highly asymmetric and multiple intersecting shear bands appeared on the sample surface over a wide range of angles.

As the orientation approached 45° the deformation and fracture sequence showed much more evidence of ductility and was typified by the early occurrence of symmetrical barreling. At later stages of the deformation, one or more major shear bands occurred at ~45° to the compression axis, Fig. 3(d) often appearing as a pair of intersecting shear bands.

At quasi-static strain rates the failure processes were essentially similar, showing a transition from longitudinal splitting to more uniform deformation followed by barreling and shear band formation. Figure 4 depicts representative samples after testing and shows the severe layer splitting noted previously in 0° samples, Fig. 4(a). The pronounced asymmetry of the 30° quasi-static sample is now clearly visible, Fig. 4(c), while the corresponding high strain-rate sample is noted to have disintegrated into numerous fragments, Fig. 4(d).

Examination in the scanning electron microscope showed that fiber fragmentation became increasingly pronounced as the misorientation increased, Fig. 5(a). Polished sections from tested samples confirmed the general observations noted above but also revealed more clearly the extensive fiber fragmentation and shear band formation that accompanied the deformation events. Also, detailed examination of the failure modes predicted by the

numerical models confirmed the general features and appearances of these deformation and fracture modes, Fig 5(b).

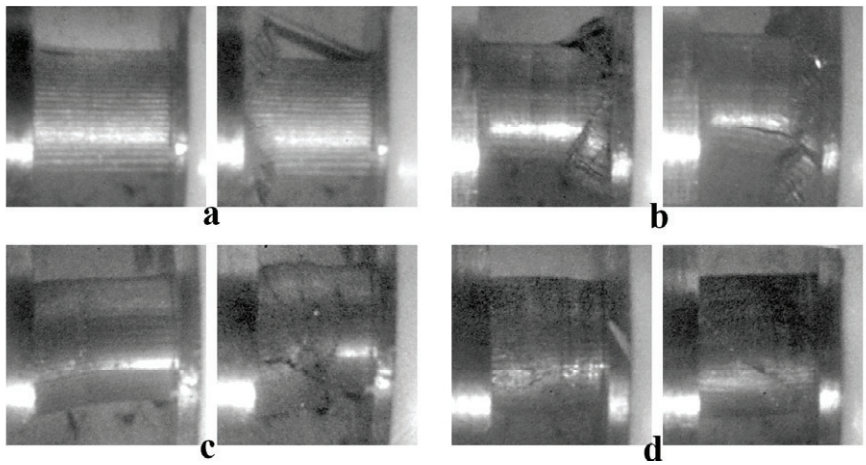

Figure 3: Selected images from high-speed camera sequences showing stages of deformation for different orientations: (a) 0°, (b) 10°, (c) 20°, (d) 40°.

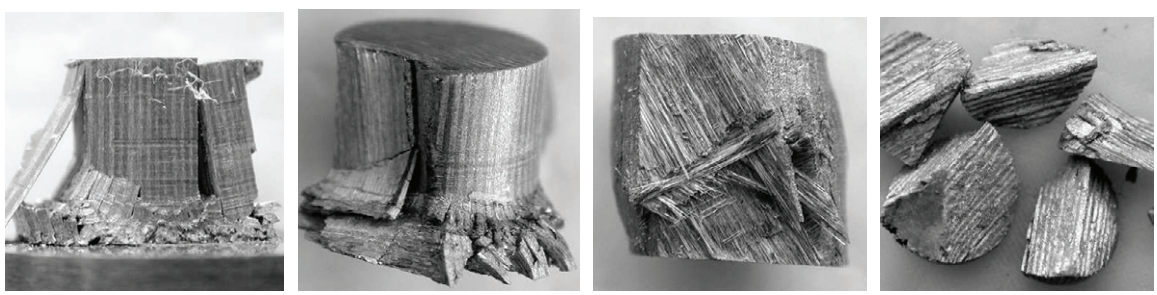

Figure 4: Macroscopic views of selected tested samples; (a) 0° quasi-static, (b) 10° high strain-rate, (c) 30° quasi-static, (d) 30° high strain-rate.

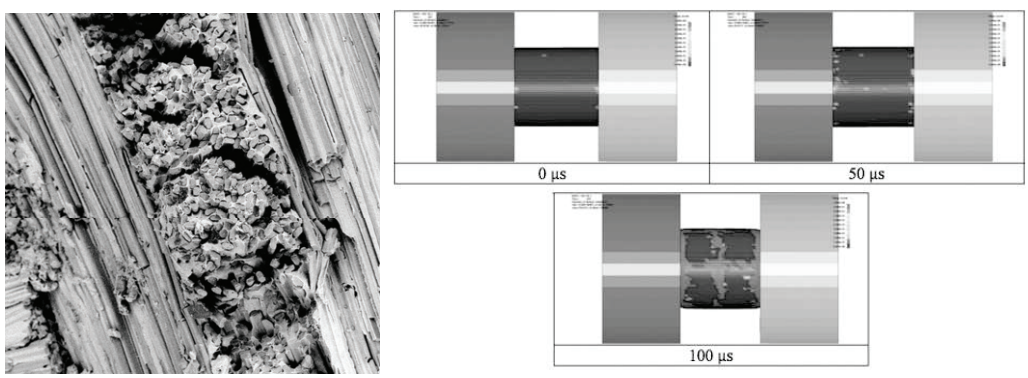

Figure. 5: (a) Scanning electron micrograph of sample tested at 30° misorientation showing layer delamination as well as fiber and bundle fragmentation: (b) sequence from numerical model showing development of fiber failure in 45° sample.

4. Discussion

A cross-ply lay-up, may be simplistically thought of as somewhat more isotropic and possibly, therefore, less sensitive to precise orientation than a unidirectionally reinforced composite. However, the primary conclusion from

the present work is that the mechanical properties of these MMC's are still very sensitive to the direction of testing and, hence, to the axes along which operational stresses are applied. The rapidity with which the fracture stresses declined at orientations away from 0/90° resembled that for unidirectional composites and led to a decrease of ~40° after a 10° deviation.

The principal consequence of this decrease in properties is that design and manufacture must be very strictly controlled in order to achieve the optimum properties. Metallographic examination of the MMC's used in this work showed that, there was a considerable spread of fiber orientation around the nominal axes. For example, the 0° fibers in the 0/90° orientation showed a distribution in which 95% were aligned within ±3° of the 0° axis, a small deviation but one which is capable of reducing the load bearing capacity of the composite by 300MPa.

A further feature of the data is that the properties were somewhat dependent upon strain rate, with quasi-statically tested samples showing consistently lower values than those tested at high strain rate. The reasons for this are complex but are not believed to reflect true strain-rate sensitivity because true strain-rate sensitivity occurs most markedly and commonly in pure metals rather than in alloys. Also, when observed, strain rate sensitivity usually occurs at strain rates significantly in excess of 10^3 s^{-1}. Instead, the apparent superiority of properties at high strain rate is believed to be due to differences in the way that the samples deformed and fractured. For example, as mentioned above, examination of the stress strain curves for the two strain-rate regimes shows that quasi-statically tested samples showed increasing ductility with increasing angular deviation and monotonically increasing curves until just before final fracture.

However, high strain-rate tested samples showed a more complex behavior in which increasing angular deviation led to more apparent ductility (defined here as strain to failure) but also led to the appearance of successive peaks and troughs. Detailed examination of the high-speed photographic sequences showed that these features correspond to progressive failure of the samples during which an initial failure event, such as layer splitting, occurred and led to a decrease in load-bearing capability. However, since the test was conducted rapidly, the fragments remained in place and were subsequently re-loaded. This sequence could be repeated several times and lead to several peaks. A further consequence of the fragments remaining in place was that, for larger angular deviations when the sample began to barrel significantly, the load-bearing area of the sample became larger and hence the maximum stresses increased.

In conclusion it has been shown that the mechanical properties of cross-ply MMC's in compression are extremely sensitive to small fiber misorientations: the sensitivity in tension is anticipated to be less but has not yet been characterized.

References

[1] Hall, I.W., Tasdemirci, A., Derrick, J., Quasi-static and high strain-rate properties of a cross-ply metal matrix composite. Materials Science and Engineering, A, 2009;**507**:93–101

[2] Cady, C.M., Gray, G.T. Influence of strain rate on the deformation and fracture response of a 6061-T6 Al-50 vol.% Al2O3 continuous-reinforced composite. Materials Science and Engineering A, 2001:**298**;56–62.

[3] Güden, M., Akil, O., Tasdemirci, A., Çiftçioglu, M., Hall, I.W., Effect of strain rate on the compressive mechanical behavior of a continuous alumina fiber reinforced ZE41A magnesium alloy based composite. Materials Science and Engineering A: **2006:**425;145–155.

[4] Deve, H.E., Compressive strength of continuous fiber reinforced aluminum matrix composites. Acta Materialia. 1997:**45**;5041–5046.

[5] Argon, A. S., in Treatise of Materials Science Technology, 1, Academic Press, (1972), 79-113.

[6] Piggott, M. R., and Wilde, P., Compressive strength of aligned steel reinforced epoxy resin. J. of Matls. Sci, 1980:**15**; 2811-2815.

[7] Hashin, Z., Failure Criteria for Unidirectional Fiber Composites. Journal of Applied Mechanics, 1980:**47**;329-334.

[8] Matzenmiller, A.L., J.; Taylor, R. L., A constitutive model for anisotropic damage in fiber-composites. Mechanics of Materials, 1995: **20(2)**;125-152.

[9] Tasdemirci, A., Kara, A., Turan, A.K., Tunusoglu, G., Guden, M., Hall, I.W., Experimental and Numerical Investigation of High Strain Rate Mechanical Behavior of a [0/45/90/- 45] Quadriaxial E-Glass/Polyester Composite, *this volume*.